Spin-orbit tuned metal-insulator transitions in single-crystal $Sr_2Ir_{1-x}Rh_xO_4$ ($0 \leqslant x \leqslant 1$)

T. F. Qi,[1] O. B. Korneta,[1] L. Li,[1] K. Butrouna,[1] V. S. Cao,[1,*] Xiangang Wan,[2] P. Schlottmann,[3] R. K. Kaul,[1] and G. Cao[1,†]

[1]*Center for Advanced Materials and Department of Physics and Astronomy, University of Kentucky, Lexington, Kentucky 40506, USA*

[2]*Department of Physics, Nanjing University, Nanjing, People's Republic of China*

[3]*Department of Physics, Florida State University, Tallahassee, Florida 32306, USA*

(Received 28 June 2012; revised manuscript received 8 August 2012; published 6 September 2012)

Sr_2IrO_4 is a magnetic insulator driven by spin-orbit interaction (SOI) whereas the isoelectronic and isostructural Sr_2RhO_4 is a paramagnetic metal. The contrasting ground states have been shown to result from the critical role of the strong SOI in the iridate. Our investigation of structural, transport, magnetic, and thermal properties reveals that substituting $4d$ Rh^{4+} ($4d^5$) ions for $5d$ Ir^{4+} ($5d^5$) ions in Sr_2IrO_4 directly reduces the SOI and rebalances the competing energies so profoundly that it generates a rich phase diagram for $Sr_2Ir_{1-x}Rh_xO_4$ featuring two major effects: (1) Light Rh doping ($0 \leqslant x \leqslant 0.16$) prompts a simultaneous and precipitous drop in both the electrical resistivity and the magnetic ordering temperature T_C, which is suppressed to zero at $x = 0.16$ from 240 K at $x = 0$. (2) However, with heavier Rh doping [$0.24 < x < 0.85$ (± 0.05)] disorder scattering leads to localized states and a return to an insulating state with spin frustration and exotic magnetic behavior that only disappears near $x = 1$. The intricacy of $Sr_2Ir_{1-x}Rh_xO_4$ is further highlighted by comparison with $Sr_2Ir_{1-x}Ru_xO_4$ where Ru^{4+} ($4d^4$) drives a direct crossover from the insulating to metallic states.

DOI: 10.1103/PhysRevB.86.125105 PACS number(s): 75.70.Tj, 71.30.+h

I. INTRODUCTION

Sr_2IrO_4 is an archetype for new physics primarily driven by the interplay of electron-electron and spin-orbit interactions (SOI).[1–3] The relativistic SOI proportional to Z^4 (Z is the atomic number) is approximately 0.4 eV in the iridate (compared to ~20 meV in $3d$ materials), and splits the t_{2g} bands into bands with $J_{\text{eff}} = 1/2$ and $J_{\text{eff}} = 3/2$, the latter having lower energy.[1,2] Since the Ir^{4+} ($5d^5$) ions provide five $5d$ electrons, four of them fill the lower $J_{\text{eff}} = 3/2$ bands, and one electron partially fills the $J_{\text{eff}} = 1/2$ band where the Fermi level E_F resides. The $J_{\text{eff}} = 1/2$ band is so narrow that even a reduced on-site Coulomb repulsion U (~0.5 eV) due to the extended nature of $5d$-electron orbitals is sufficient to open a small gap ($\leqslant$0.1 eV) supporting the insulating state.[1,2] Most recently, an x-ray absorption spectroscopy study indicates a mixing of the $J_{\text{eff}} = 1/2$ and $J_{\text{eff}} = 3/2$ bands as a result of exchange interactions (~0.2 eV) and a tetragonal crystal electric field (CEF) (~0.075 eV).[4] Nevertheless, the larger the SOI and the narrower the band is, the smaller U is needed for a SOI-related insulating state,[5] in which SOI, Coulomb interactions, tetragonal CEF, and Hund's coupling J_H become so comparable that they vigorously compete with each other, setting a new balance between the relevant energies that can drive new exotic states.[1–18]

In contrast, the isoelectronic $4d$-based Sr_2RhO_4 with Rh^{4+} ($4d^5$) ions with five $4d$ electrons has a weaker SOI (~0.16 eV), thus a smaller splitting between the $J_{\text{eff}} = 1/2$ and $J_{\text{eff}} = 3/2$ bands that are more evenly filled by the five $4d$ electrons.[5,15–18] The weaker SOI combined with more effectively screened Coulomb interactions between O $2p$ and Rh $4d$ electrons favors a metallic state.[15] Indeed, Sr_2RhO_4 is a paramagnetic, correlated metal[16–18] sharply contrasting the magnetic insulator Sr_2IrO_4 that orders at $T_C = 240$ K.[6,19–21] In addition, comparisons of Sr_2RhO_4 with another $4d$-based compound, Sr_2RuO_4, a p-wave superconductor,[22] reveal that the impact of the SOI strongly depends on the detailed band structure near the Fermi surface E_F, the Coulomb interactions, and the lattice distortions.[7,15,23,24] The t_{2g} bands in Sr_2RhO_4 near E_F are less dispersive than those in Sr_2RuO_4, therefore more susceptible to the SOI-induced band shifts near E_F than in Sr_2RuO_4 despite the similar strength of the SOI in both materials.[23] This is in part because the Ru^{4+} ($4d^4$) ion has four $4d$ electrons instead of five; Ru doping therefore adds holes to the bands.

Both Sr_2IrO_4 and Sr_2RhO_4 are not only isoelectronic but also isostructural with a crystal structure similar to that of Sr_2RuO_4 and La_2CuO_4.[16] A unique and important structural feature shared by both Sr_2IrO_4 and Sr_2RhO_4 is that they crystallize in a reduced tetragonal structure with space-group $I4_1/acd$ due to a rotation of the IrO_6 or RhO_6 octahedra about the c axis by ~12° or ~9.7°, respectively, resulting in a larger unit cell by $\sqrt{2} \times \sqrt{2} \times 2$,[16,19–21] as compared to the undistorted cell.

That the two isostructural and isoelectronic compounds exhibit the sharply contrasting physical properties underscores the critical role SOI plays in determining the ground state of the iridate. In this work, we tune the ground state via reducing SOI by substituting Rh^{4+} ($4d^5$) for Ir^{4+} ($5d^5$) in Sr_2IrO_4, i.e., in single-crystal $Sr_2Ir_{1-x}Rh_xO_4$ ($0 \leqslant x \leqslant 1$). As schematically illustrated in Fig. 1(a), the Rh substitution, unlike other chemical substitutions, directly reduces the SOI, thus the splitting between the $J_{\text{eff}} = 1/2$ and $J_{\text{eff}} = 3/2$ bands but without obviously altering the band filling. Hence, the system remains tuned at the Mott instability and is very susceptible to disorder scattering which gives rise to localization. For comparison and contrast, we also substitute Ru^{4+} ($4d^4$) for Ir^{4+} ($5d^5$) in Sr_2IrO_4, i.e., $Sr_2Ir_{1-x}Ru_xO_4$ ($0 \leqslant x \leqslant 1$), where Ru not only reduces the SOI but also fills the t_{2g} bands with holes, which lowers E_F, thus moving the system away from the Mott instability. Disorder scattering is then less relevant, and Ru doping systematically drives the system to a robust metallic state. The anticipated underlying effects of Ru doping on the $J_{\text{eff}} = 1/2$ and $J_{\text{eff}} = 3/2$ bands are also schematically illustrated in Fig. 1(a). The doping profoundly alters the

 ©2012 American Physical Society

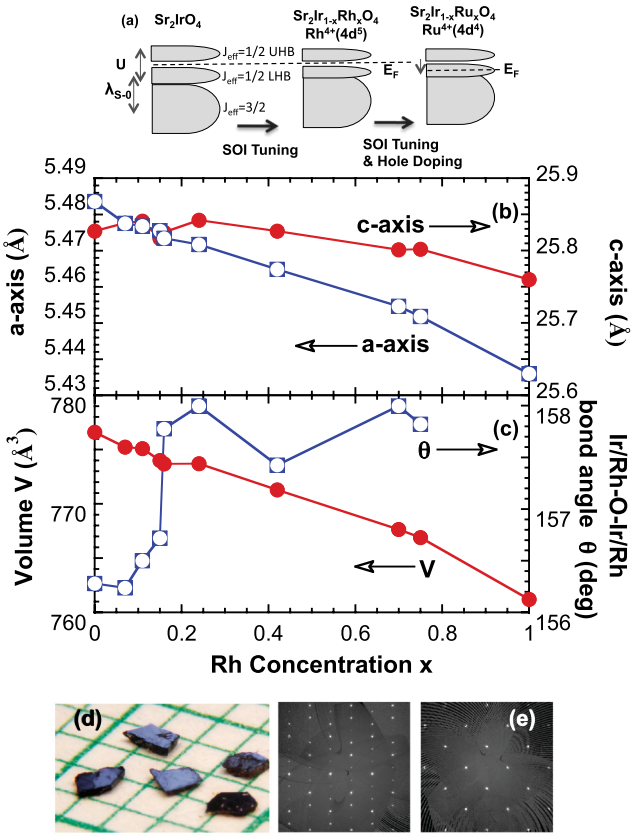

FIG. 1. (Color online) (a) The schematics for the effects of Rh and Ru doping on the $J_{\rm eff} = 1/2$ and $J_{\rm eff} = 3/2$ bands; the Rh concentration x dependence at 90 K of (b) the lattice parameters' a and c axes (right scale), and (c) the unit cell volume V and the Ir-O-Ir angle θ (right scale). (d) Some representative single-crystal $Sr_2Ir_{1-x}Rh_xO_4$ and (e) their Bragg diffraction peaks ([100] and [001] directions); note the highly ordered crystal structure.

balance between the competing local energies; namely, the SOI is weakened, while the tetragonal CEF and the Hund's coupling J_H are increased. In addition, the Rh and Ir atoms are randomly distributed over the octahedra, hindering the hopping of the d electrons because of a mismatch of the energy levels and a mismatch of the rotation of the octahedra. The resulting disorder scattering gives rise to localized states. The combined effects produces a rich T-x phase diagram in $Sr_2Ir_{1-x}Rh_xO_4$ featuring two major effects: (1) Light Rh doping ($0 \leqslant x \leqslant 0.16$) effectively reduces the SOI and prompts a simultaneous and precipitous drop in both the electrical resistivity $\rho(T)$ and the magnetic ordering temperature T_C, which becomes zero at $x = 0.16$ from 240 K at $x = 0$. The results indicate that the Rh concentration does provide a degree of control on the splitting between $J_{\rm eff} = 1/2$ and $J_{\rm eff} = 3/2$ bands. (2) However, heavier Rh doping [$0.24 < x < 0.85$ (± 0.05)] increases localization effects in the system which fosters a return to an insulating state with anomalous magnetic behavior occurring below 0.3 K that only disappears near $x = 1$. The magnetic state is expected to arise from the strong competition between antiferromagnetic (AFM) and ferromagnetic (FM) coupling that causes strong spin frustration. A recent optical study [26] on thin-film $Sr_2Ir_{1-x}Rh_xO_4$ with x up to 0.26 is qualitatively consistent with some of our results. However, the present work addresses structural and physical properties of *bulk single-crystal* $Sr_2Ir_{1-x}Rh_xO_4$ with x *ranging from* 0 *to* 1.

II. EXPERIMENTAL

The single crystals studied were grown from off-stoichiometric quantities of $SrCl_2$, $SrCO_3$, IrO_2, and RhO_2 or RuO_2 using self-flux techniques. Similar technical details are described elsewhere.[6,8–10] The size of the single crystals is as large as $1.0 \times 1.0 \times 0.2\ \rm cm^3$ [see Fig. 1(d)]. The structures of $Sr_2Ir_{1-x}Rh_xO_4$ and $Sr_2Ir_{1-x}Ru_xO_4$ were determined using a Nonius Kappa CCD x-ray diffractometer at 90 K and 295 K. Structures were refined by full-matrix least squares using the SHELX-97 programs.[27] The standard deviations of all lattice parameters and interatomic distances are smaller than 0.1%. The structure of the single crystals studied is highly ordered, as evidenced by sharp and bright Bragg diffraction spots along the [100] and [001] directions, respectively, in Fig. 1(e). We also checked the atom site occupancy factor on oxygen sites by running a test in which the oxygen occupancies were allowed to refine freely. They are all refined with full-occupancy factors, suggesting that no clear oxygen vacancy was found from the refinement. Chemical compositions of the single crystals were determined using a combined unit of Hitachi/Oxford SwiftED 3000 for energy dispersive x-ray (EDX) spectroscopy. The specific heat, $C(T)$, was measured down to 50 mK whereas the resistivity, $\rho(T)$, and the magnetization, $M(T)$, were measured between 1.7 K and 400 K using a Quantum Design (QD) 7T SQUID magnetometer and a QD 14T Physical Property Measurement System, respectively.

III. RESULTS AND DISCUSSION

Substituting Rh^{4+} for Ir^{4+} results in a nearly uniform reduction in the lattice parameters' a c axes and the unit cell V that is shrunk by ~2%, as shown in Figs. 1(b) and 1(c). This behavior is expected for Rh^{4+} doping because the ionic radius of Rh^{4+} (0.600 Å) is smaller than that of Ir^{4+} (0.625 Å). [An increase in the lattice parameters would be anticipated instead for Rh^{3+} ($4d^6$) doping because of the larger ionic radius of Rh^{3+}, 0.670 Å.] The a axis is compressed by 0.87% whereas the c axis only by 0.26%, which enhances the tetragonal CEF. In addition, the Ir-O-Ir bond angle θ increases significantly near $x = 0.16$, indicating a less distorted lattice for $x > 0.16$. It is already established that θ is critical to the electronic and magnetic structure of Sr_2IrO_4.[7–10,25]

Rh doping effectively suppresses the magnetic transition T_C from 240 K at $x = 0$ to zero at $x = 0.16$, as shown in Figs. 2(a), 2(b), and 2(c). With increasing x, the c-axis magnetization M_c becomes relatively stronger at $\mu_0 H = 0.1$ T. This is consistent with the reduced magnetic anisotropy in isothermal magnetization $M(H)$ for $x = 0.11$ at $T = 1.7$ K and near $\mu_0 H = 1$ T, as shown in the inset in Fig. 2(b); the ratio M_a/M_c at lower fields (<2 T) is significantly weaker for $x = 0.11$ than for $x = 0$.[10] This change could be due to a change in the relative strength of SOI and tetragonal CEF as an enhanced tetragonal CEF due to the increased c/a ratio [Fig. 1(b)] encourages a spin configuration along the c axis.[7] The magnetic data in Fig. 2 were first fitted to a Curie-Weiss

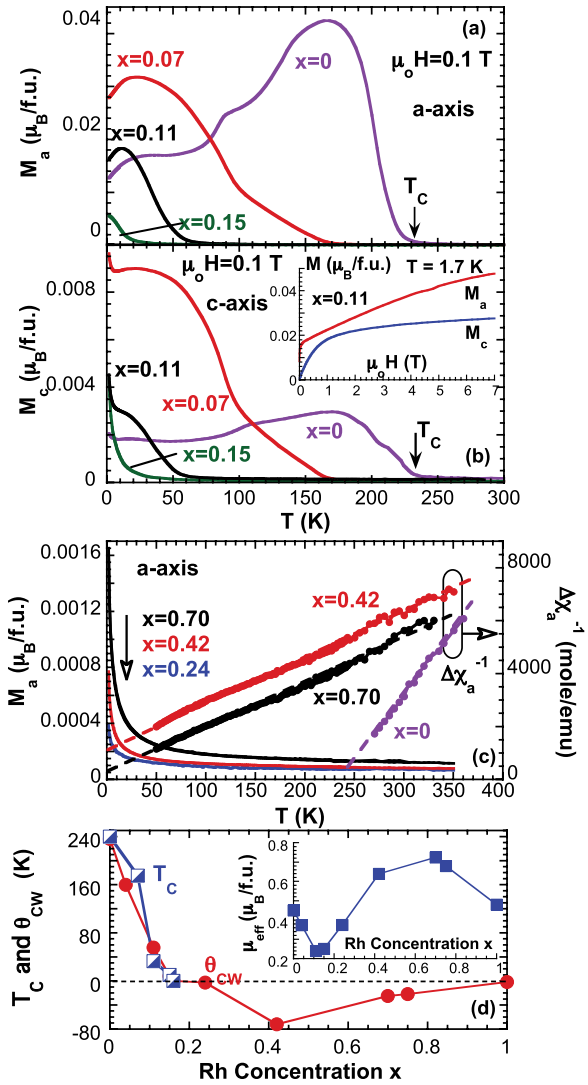

FIG. 2. (Color online) The temperature dependence at $\mu_0 H = 0.1$ T of the magnetization (a) M_a, (b) M_c for $0 \leqslant x \leqslant 0.15$ and isothermal magnetization M_a and M_c for $x = 0.11$ at $T = 1.7$ K (inset); and (c) M_a for $0.24 \leqslant x \leqslant 0.75$ and $\Delta\chi_a^{-1}$ (right scale) for $x = 0$, 0.42, and 0.70. (d) The Rh concentration x dependence of T_C and θ_{CW}, and the magnetic effective moment μ_{eff} (inset).

law $\chi = \chi_0 + C/(T + \theta_{CW})$ for a temperature range of 50–350 K for $x > 0.16$ (χ_0 is a temperature-independent constant, θ_{CW} the Curie-Weiss temperature, and C the Curie constant); and we then used χ_0 to obtain $\Delta\chi = C/(T + \theta_{CW})$ and plotted the data in terms of $\Delta\chi^{-1}$ vs T, as shown in Fig. 2(c) (right scale). θ_{CW} tracks the rapidly decreasing T_C for $0 \leqslant x \leqslant 0.16$, and becomes nearly zero at $x = 0.16$ and then changes its sign from positive to negative as x further increases. It is remarkable that θ_{CW} is -72 K at $x = 0.42$ and then becomes -2 K at $x = 1$, as shown in Fig. 2(d). Since θ_{CW} measures the strength of the magnetic interaction, such a large absolute value of θ_{CW} ($= -72$ K) in a system without magnetic ordering above 0.3 K (magnetic order below 0.3 K is observed and discussed below) implies a strong suppression of magnetic ordering or spin frustration. It becomes conceivable that both the disappearance of the magnetic order at $x = 0.16$ and the appearance of the spin frustration at higher x are a consequence of the Rh and Ir disorder and the changes in local energies with x, such as the SOI, the noncubic CEF, and the enhanced Hund's rule coupling, which intensify the competition between AFM and FM couplings. In addition, the magnetic susceptibility $\chi(T)$ for $0.24 \leqslant x \leqslant 0.75$ below 40 K follows a power law, $\chi(T) \sim T^{-\alpha}$ with α increasing with x from 0.35 to 0.57, suggesting strong spin interaction among unscreened spins even at low temperatures.

The Rh doping unexpectedly generates three doping regions having distinct transport behavior, that is, region I: $0 \leqslant x \leqslant 0.24$, region II: $0.24 < x < 0.85$ (± 0.05), and region III: 0.85 (± 0.05) $< x \leqslant 1$. Region III represents a metallic state occurring in a very narrow region close to $x = 1$, i.e., Sr_2RhO_4, that is thoroughly discussed in Ref. 17. Here we focus on regions I and II, which are discussed separately below.

Region I, $0 \leqslant x \leqslant 0.24$. The electrical resistivity ρ(T) for the a and c axes drastically reduces by nearly six orders of magnitude at low temperatures from $\sim 10^6$ Ω cm at $x = 0$ to ~ 1 Ω cm at $x = 0.07$, as shown in Fig. 3(a). For $0.07 < x \leqslant 0.24$, the a-axis resistivity $\rho_a(T)$ above 50 K exhibits metallic-like behavior, $d\rho_a/dT > 0$, and a largely reduced magnitude of $\rho_a(T)$ ranging from 10^{-3} to 10^{-1} Ω cm [see Fig. 3(b)]. $d\rho_a/dT > 0$ becomes most obvious at $x = 0.11$. The corresponding c-axis resistivity $\rho_c(T)$ shows a slightly larger magnitude, but with $d\rho_c/dT$ remaining negative, as

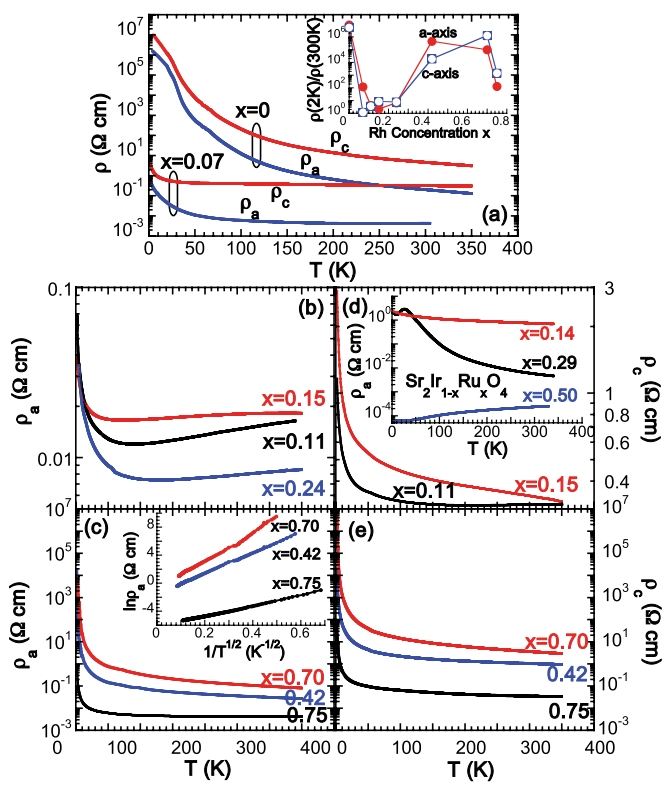

FIG. 3. (Color online) The temperature dependence for $Sr_2Ir_{1-x}Rh_xO_4$ of (a) the resistivity ρ for $x = 0$ and 0.07; (b) the a-axis resistivity ρ_a for $x = 0.11$, 0.15, and 0.24; (c) ρ_a for $x = 0.42$, 0.70, and 0.75; (d) the c-axis resistivity ρ_c for $x = 0.11$ and 0.15; (e) ρ_c for $x = 0.42$, 0.70, and 0.75. Inset in (a): The ratio of $\rho(2\text{ K})/\rho(300\text{ K})$ vs x; inset in (c): ln ρ_a vs $T^{-1/2}$; inset in (d): ρ_a vs T for $Sr_2Ir_{1-x}Ru_xO_4$, where a robust metallic state occurs at $x = 0.50$.

shown in Fig. 3(d). Since the bond angle θ, which is critical to electron hopping in general, remains essentially unchanged until $x > 0.16$ [Fig. 1(c)] and the Rh doping adds no holes or electrons to the bands, the drastic reductions in $\rho_a(T)$ and $\rho_c(T)$ may be primarily due to the weakened SOI. In addition, the vanishing magnetic state in this doping range may also help reduce the band gap because the internal magnetic field lifts the degeneracy along the edge of the AF Brillouin zone, thus facilitating the SOI to open a full gap in the presence of U.[5] Both $\rho_a(T)$ and $\rho_c(T)$ exhibit a noticeable upturn below 50 K indicating that a low-temperature metallic state is not fully realized although $\rho_a(T)$ and $\rho_c(T)$ are radically reduced by six orders of magnitude. It is also noted that $\rho_a(T)$ for $x = 0.24$ follows variable range hopping (VRH) model, $\rho \sim \exp(1/T)^{1/2}$, below 50 K. It implies that Anderson localization comes into play at $x = 0.24$. The persisting nonmetallic state below 50 K suggests that the band gap is not fully closed with conducting states despite the weakened SOI and the diminishing internal magnetic field. It is interesting to see that 14% of Ru doping, which not only reduces SOI but also adds holes to the bands, also fails to induce a metallic state [see inset in Fig. 3(d)].

Region II, $0.24 < x < 0.85$ (± 0.05). If the reduction of SOI were the only mechanism, a more metallic state would be expected with increasing x. However, both $\rho_a(T)$ and $\rho_c(T)$ increase significantly, reaching 10^5 and 10^7 Ω cm, respectively, at low temperatures for $x = 0.70$ before dropping again to 10^{-1} Ω cm for $x = 0.75$, as shown in Figs. 3(c) and 3(e). No metallic behavior ($d\rho/dT > 0$) is observed in the entire temperature range measured for $x = 0.42$, 0.70, and 0.75. The insulating state occurring in this region is the consequence of localization due to disorder on the Rh/Ir site in the alloy. ρ for these Rh concentrations fits the VRH $\rho \sim \exp(1/T)^{1/2}$ for $2 < T < 100$ K, suggesting that Anderson localization due to disorder becomes significant in the presence of Coulomb interaction.[28] However, it cannot be ruled out that there might exist clusters of Rh-doped areas although the single crystals studied are highly ordered [Fig. 1(e)]. It sharply contrasts the well-established metallic state in $Sr_2Ir_{1-x}Ru_xO_4$ with $x = 0.50$ [inset of Fig. 3(d)]. It is important to note that our oxygenated single crystals with $x = 0.42$, 0.70, and 0.75 exhibit essentially identical magnitude and temperature dependence of $\rho_a(T)$ and $\rho_c(T)$; this result rules out an insulating state that might be induced by oxygen deficiency. Indeed, the x-ray refinement already confirms no discernible oxygen deficiency in the single crystals studied.

The ratio of $\rho(2\text{ K})/\rho(300\text{ K})$ for both $\rho_a(T)$ and $\rho_c(T)$ qualitatively captures the change of transport properties with Rh concentration x [see inset in Fig. 3(c)]. The initial, precipitous drop in the ratio from $\sim 10^6$ at $x = 0$ to ~ 1 near $x = 0.16$ signals the rapidly growing metallic-like state. The ratio rises again at $x > 0.24$, marking the return to an insulating state, before falling back for $x > 0.70$. The effective moment μ_{eff} essentially tracks the change of the ratio of $\rho(2\text{ K})/\rho(300\text{ K})$. This reflects the association of localized states with the magnetic degrees of freedom [inset in Fig. 2(d)].

The temperature dependence of the specific heat C for various x is shown in Fig. 4(a). Fitting the data to $C(T) = \gamma T + \beta T^3$ for $10 < T < 50$ K yields the coefficient for the electronic contribution to $C(T)$, γ, that systematically

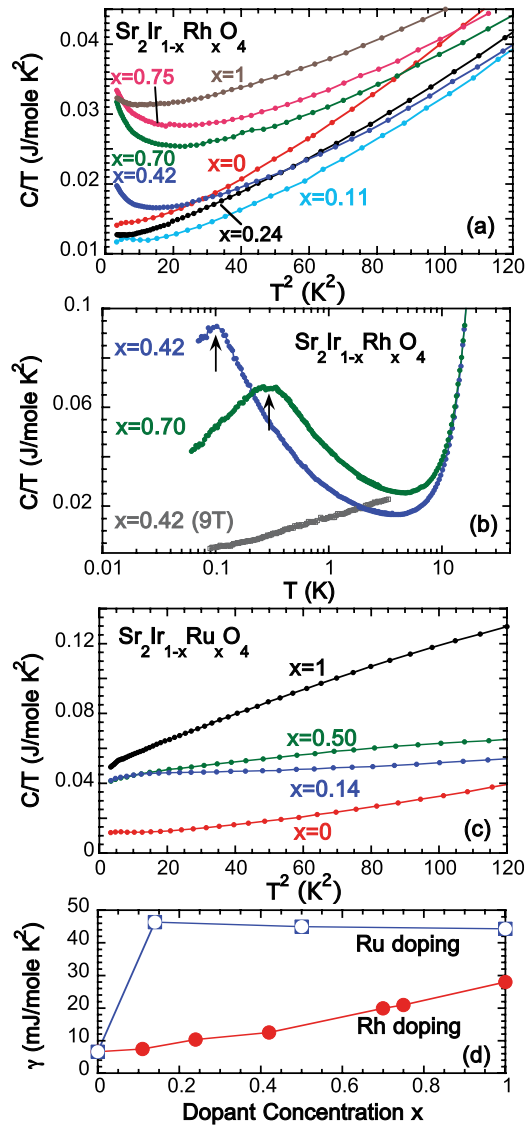

FIG. 4. (Color online) (a) The specific heat $C(T)/T$ vs T^2 for $Sr_2Ir_{1-x}Rh_xO_4$; (b) $C(T)/T$ vs T for 50 mK $< T <$ 20 K at $\mu_0 H = 0$ for $x = 0.42$ and 0.70, and 9 T for $x = 0.42$; (c) $C(T)/T$ vs T^2 for $Sr_2Ir_{1-x}Ru_xO_4$ for comparison; (d) γ vs x for $Sr_2Ir_{1-x}Rh_xO_4$ and $Sr_2Ir_{1-x}Ru_xO_4$.

increases with x from 7 mJ/mole K^2 at $x = 0$ to 30 mJ/mole K^2 at $x = 1$. The increased γ for the insulating region $0.24 < x \leqslant 0.75$ may be a result of the states that are localized due to disorder in the gap, which give rise to a finite density of states [Fig. 4(d)]. Since Rh is not a dopant in the conventional sense, the conventional picture of hydrogen-like impurities does not apply. However, any breaking of the translational invariance of the system (such as Rh ions) necessarily introduces a bound state in the gap of the semiconductor. This leads to a gradual filling of the gap with x. Remarkably, $C(T)/T$ exhibits a pronounced peak near $T_M = 100$ mK and 280 mK for $x = 0.42$ and 0.70, respectively, which can be completely suppressed by a magnetic field H of 9 T [Fig. 4(b)]. This anomaly signals a transition to a low-T spin order from a higher-T spin frustration characterized by a frustration parameter $f = |\theta_{\text{CW}}|/T_M = |-72|/0.1 = 720$ for

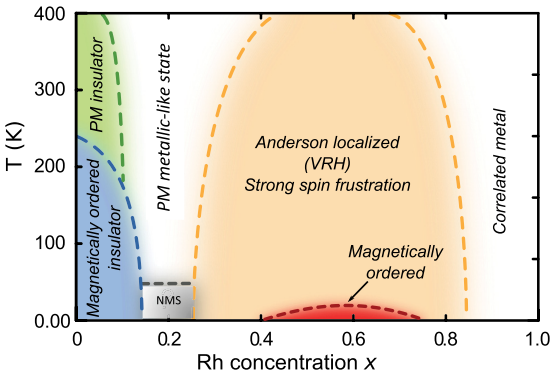

FIG. 5. (Color online) The phase diagram for $Sr_2Ir_{1-x}Rh_xO_4$ generated based on the data presented above. Note that PM stands for paramagnetic and NMS nonmetallic state.

$x = 0.42$, for example. In contrast, $Sr_2Ir_{1-x}Ru_xO_4$ behaves more normally [Fig. 4(c)], yielding γ considerably larger than that for $Sr_2Ir_{1-x}Rh_xO_4$ [Fig. 4(d)], which is consistent with the robust metallic state.

Figure 5 shows a phase diagram for $Sr_2Ir_{1-x}Rh_xO_4$ generated based on the data presented above which summarizes the central findings of this study. The initial Rh doping effectively reduces the SOI, or the splitting between the $J_{\rm eff} = 1/2$ and $J_{\rm eff} = 3/2$ bands, and alters the relative strength of the SOI and the tetragonal CEF that dictates the magnetic state, which, in turn, affects the band gap near E_F. In addition, the Rh doping also enhances the Hund's rule coupling that competes with the SOI, and prevents the formation of the $J_{\rm eff} = 1/2$ state.[5] It is these SOI-induced changes that account for the simultaneous, precipitate decrease in $\rho(T)$ and T_C that vanishes at $x = 0.16$. As x increases further, the Rh/Ir disorder on the transition-metal site determines the properties of the system. There is an energy level mismatch for the Rh and Ir sites that makes the hopping of the carriers between an octahedron containing a Rh atom and one with an Ir ion more difficult and also changes the orientation angles of the octahedra. The randomness of the Rh/Ir occupations gives rise to Anderson localization and an insulating state for $0.24 < x < 0.85$ (± 0.05). In addition, the SOI may no longer be strong enough to support the $J_{\rm eff} = 1/2$ insulating state and the Hund's rule coupling is enhanced (on the Rh sites), hence further strengthening the competition between AFM and FM couplings. As a result of this competition, spin frustration arises at intermediate temperatures. The occurrence of a spin-ordered state below 0.3 K along with the high $\theta_{\rm CW}$ corroborates the frustrated state. These effects diminish with disappearing disorder when x approaches 1, where the weakened SOI is comparable to other relevant energies yielding a metallic state. This point is qualitatively consistent with the recent theoretical studies for Sr_2RhO_4.[15,20,21]

In contrast, there is no discernible effect due to disorder in $Sr_2Ir_{1-x}Ru_xO_4$. While for isoelectronic Rh substitution the system always remains in the proximity to the Mott condition for an insulator, each Ru atom adds one hole, giving rise to a higher density of states near E_F and hence supporting a more robust metallic state in Sr_2RuO_4. Under these circumstances disorder in the alloy plays a less relevant role.

ACKNOWLEDGMENTS

G.C. is very grateful to G. Khaliulin, X. Dai, Y. B. Kim, H. Y. Kee, and G. Jackeli for enlightening discussions. This work was supported by the NSF through Grants No. DMR-0856234 (G.C.), No. EPS-0814194 (G.C., R.K.K.), and No. DMR-1056536 (R.K.K.) and by the Department of Energy through Grant No. DE-FG02-98ER45707 (P.S.).

*High school student on internship, Paul Lawrence Dunber High School, Lexington, Kentucky 40513, USA.
†Corresponding author: cao@uky.edu

[1] B. J. Kim, Hosub Jin, S. J. Moon, J.-Y. Kim, B.-G. Park, C. S. Leem, Jaejun Yu, T. W. Noh, C. Kim, S.-J. Oh, V. Durairai, G. Cao, and J.-H. Park, Phys. Rev. Lett. **101**, 076402 (2008).
[2] S. J. Moon, H. Jin, K. W. Kim, W. S. Choi, Y. S. Lee, J. Yu, G. Cao, A. Sumi, H. Funakubo, C. Bernhard, and T. W. Noh, Phys. Rev. Lett. **101**, 226401 (2008).
[3] B. J. Kim, H. Ohsumi, T. Komesu, S. Sakai, T. Morita, H. Takagi, and T. Arima, Science **323**, 1329 (2009).
[4] D. Haskel, G. Fabbris, Mikhail Zhernenkov, P. P. Kong, C. Jin, G. Cao, and M. van Veenendaal, Phys. Rev. Lett. **109**, 027204 (2012).
[5] Hiroshi Watanabe, Tomonori Shirakawa, and Seiji Yunoki, Phys. Rev. Lett. **105**, 216410 (2010).
[6] G. Cao, J. Bolivar, S. McCall, J. E. Crow, and R. P. Guertin, Phys. Rev. B **57**, R11039 (1998).
[7] G. Jackeli and G. Khaliulin, Phys. Rev. Lett. **102**, 017205 (2009).
[8] S. Chikara, O. Korneta, W. P. Crummett, L. E. DeLong, P. Schlottmann, and G. Cao, Phys. Rev. B **80**, 140407 (R) (2009).
[9] O. B. Korneta, Tongfei Qi, S. Chikara, S. Parkin, L. E. DeLong, P. Schlottmann, and G. Cao, Phys. Rev. B **82**, 115117 (2010).
[10] M. Ge, T. F. Qi, O. B. Korneta, L. E. De Long, P. Schlottmann, and G. Cao, Phys. Rev. B **84**, 100402(R) (2011).
[11] I. Franke, P. J. Baker, S. J. Blundell, T. Lancaster, W. Hayes, F. L. Pratt, and G. Cao, Phys. Rev. B **83**, 094416 (2011).
[12] Fa Wang and T. Senthil, Phys. Rev. Lett. **106**, 136402 (2011).
[13] D. Hsieh, F. Mahmood, D. Torchinsky, G. Cao, and N. Gedik, Phys. Rev. B **86**, 035128 (2012).
[14] Q. Wang, Y. Cao, J. A. Waugh, T. F. Qi, O. B. Korneta, G. Cao, and D. S. Dessau (unpublished).
[15] Cyril Martins, Markus Aichhorn, Loig Vaugier, and Silke Biermann, Phys. Rev. Lett. **107**, 266404 (2011).
[16] M. A. Subramanian, M. K. Crawford, R. L. Harlow, T. Ami, J. A. Fernandez-Baca, Z. R. Wang, and D. C. Johnston, Physica C **235**, 743 (1994).
[17] R. S. Perry, F. Baumberger, L. Balicas, N. Kikugawa, N. J. Ingle, A. Rost, J. F. Mercure, Y. Maeno, Z. X. Shen, and A. P. Mackenzie, New J. Phys. **8**, 175 (2006).

[18]S. J. Moon, M. W. Kim, K. W. Kim, Y. S. Lee, J.-Y. Kim, J.-H. Park, B. J. Kim, S.-J. Oh, S. Nakatsuji, Y. Maeno, I. Nagai, S. I. Ikeda, G. Cao, and T. W. Noh, Phys. Rev. B **74**, 113104 (2006).

[19]Q. Huang, J. L. Soubeyroux, O. Chmaissen, I. Natali Sora, A. Santoro, R. J. Cava, J. J. Krajewski, and W. F. Peck, Jr., J. Solid State Chem. **112**, 355 (1994).

[20]R. J. Cava, B. Batlogg, K. Kiyono, H. Takagi, J. J. Krajewski, W. F. Peck, Jr., L. W. Rupp, Jr., and C. H. Chen, Phys. Rev. B **49**, 11890 (1994).

[21]M. K. Crawford, M. A. Subramanian, R. L. Harlow, J. A. Fernandez-Baca, Z. R. Wang, and D. C. Johnston, Phys. Rev. B **49**, 9198 (1994).

[22]Y. Maeno, H. Hashimoto, K. Yoshida, S. Nishizaki, T. Fujita, J. G. Bednorz, and F. Lichtenberg, Nature (London) **372**, 532 (1994).

[23]M. W. Haverkort, I. S. Elfimov, L. H. Tjeng, G. A. Sawatzky, and A. Damascelli, Phys. Rev. Lett. **101**, 026406 (2008).

[24]Guo-Qiang Liu, V. N. Antonov, O. Jepsen, and O. K. Andersen, Phys. Rev. Lett. **101**, 26408 (2008).

[25]S. J. Moon, Hosub Jin, W. S. Choi, J. S. Lee, S. S. A. Seo, J. Yu, G. Cao, T. W. Noh, and Y. S. Lee, Phys. Rev. B **80**, 195110 (2009).

[26]J. S. Lee, Y. Krockenberger, K. S. Takahashi, M. Kawasaki, and Y. Tokura, Phys. Rev. B **85**, 035101 (2012).

[27]G. M. Sheldrick, Acta Crystallogr. Sect. A **64**, 112 (2008).

[28]Nevill Mott, *Metal-Insulator Transition* (Taylor & Francis, London, 1990), p. 52.